ANISOTROPIC ROTATION OF BACTERIORHODOPSIN IN LIPID MEMBRANES

COMPARISON OF THEORY WITH EXPERIMENT

RICHARD J. CHERRY AND ROBIN E. GODFREY, *Laboratorium für Biochemie, Eidgenössische Technische Hochschule, ETH-Zentrum, CH-8092 Zürich, Switzerland*

ABSTRACT Rotational diffusion of bacteriorhodopsin in dimyristoyl phosphatidylcholine vesicles has been measured at different temperatures and lipid:protein ratios by the technique of flash-induced transient linear dichroism. The data are used to evaluate critically the theory of anisotropy decay due to protein rotation in the lipid bilayer. The theoretical model assumes that rotation of the protein occurs only around the membrane normal. Under conditions favoring completely monomeric bacteriorhodopsin, namely at molar lipid:protein ratios $>\sim 100$ and for temperatures sufficiently above the lipid phase transition, it is found that the theoretical model provides an excellent description of the experimental data. Curve-fitting analyses of the experimental decay curves show that the retinal is oriented at an angle of 78 ± 2° with respect to the membrane normal. Between 25 and 37°C, the protein rotates with a relaxation time of 15 ± 5 μs in the lipid liquid crystalline phase, corresponding to a membrane viscosity of 3.7 ± 1.3 P. The curve analysis also provides a sensitive test for the presence of protein aggregates in the lipid bilayer.

INTRODUCTION

In recent years considerable interest has been directed towards an understanding of the mobility of membrane proteins (1), particularly within the context of a fluid lipid bilayer model (2) for biological membranes. Such studies may provide important information on the relationship between mobility and function of membrane components, and on their structural arrangement in the cell membrane (for a recent review, see reference 1).

Experimental advances in the measurement of protein rotational diffusion by photoinduced transient linear dichroism (3, 4), time-resolved phosphorescence depolarization (5, 6), or saturation transfer electron paramagnetic resonance (7, 8) have complemented similar developments in the determination of lateral diffusion coefficients (9, 10). To evaluate quantitatively the information available from transient dichroism experiments it is important to have a suitable model describing protein rotation that can be critically tested in a well defined system. The application of such a model to more complex situations should help characterize, for example, protein aggregation and internal protein flexibility.

In the work reported here, we investigate the conditions under which the theory for anisotropic protein rotation in a lipid bilayer conforms to the results of rotational diffusion experiments with a single protein, bacteriorhodopsin (BR), in a reconstituted lipid vesicle system. BR is ideally suited for this purpose. There is a wealth of information on its structure, both in the native purple membrane (11) and in reconstituted systems (12); it contains an

intrinsic chromophore, retinal, which takes part in a photochemical cycle of duration ~10 ms, which may be used for the flash-induced dichroism measurements; and it may be readily obtained in an essentially monomeric form in lipid vesicles (12).

In addition to testing theoretical predictions, the present experiments also provide information on the self-aggregation of BR as a function of temperature and protein concentration.

MATERIALS AND METHODS

BR was purified from *Halobacterium halobium* (strain R_1M_1) and reconstituted into lipid vesicles with dimyristoylphosphatidylcholine (DMPC, Fluka A.G. Buchs, Switzerland) by the Triton X-100 solubilization-dialysis procedure described previously (12). Various lipid:protein (L:P) molar ratios, between 50 and 250, were obtained by the addition of the requisite amount of phospholipid to the solubilized protein. Protein content in the reconstituted vesicles was determined by the Lowry procedure (13), with the appropriate correction (14), and phospholipid content by phosphorous analysis (15). The actual L:P ratios were slightly higher than these phosphorous-based values since some endogenous lipids, consisting of sulpholipids and glycolipids, are incorporated in the vesicles (16). Samples used for flash photolysis measurements typically contained 0.5 mg protein/ml. All measurements were made on the light-adapted BR in which the retinal chromophore is in the all-*trans* conformation (11).

The rotational diffusion of BR in DMPC vesicles was investigated with the flash photolysis apparatus described previously (4) (Fig. 1). The sample was excited by a vertically-polarized 540-nm laser pulse from an Electro-Photonics model 43 dye laser (Electro-Photonics Ltd Belfast, N. Ireland). Measurements of the transient intensity changes at 570 nm, due to ground state depletion, polarized parallel and perpendicular to the exciting polarization, were obtained simultaneously with two photomultipliers. The signals were amplified and averaged with a Datalab DL 102A signal averager (Datalab Ltd, Mitchem, England). The digitized decay curves were transferred to a Hewlett-Packard 9825A desk-top computer (Hewlett-Packard Co., Palo Alto, Calif.), where the intensity changes were converted to absorbance

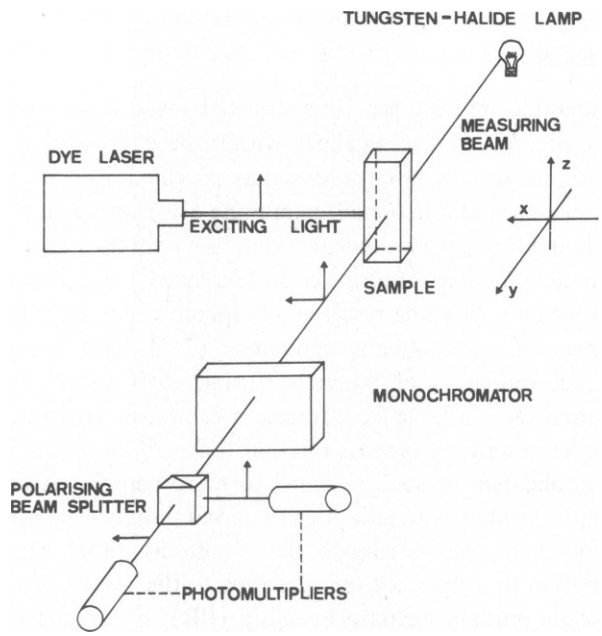

FIGURE 1 Schematic diagram of flash photolysis apparatus.

changes $\Delta A_\parallel(t)$, $\Delta A_\perp(t)$ polarized parallel and perpendicular, respectively, to the exciting polarization, and the anisotropy parameter $r(t)$ calculated as follows: (17):

$$r(t) = \frac{\Delta A_\parallel(t) - \Delta A_\perp(t)}{\Delta A_\parallel(t) + 2\Delta A_\perp(t)}. \tag{1}$$

$r(t)$ was immediately plotted against t on a Hewlett-Packard 9862A plotter for each measurement, to provide rapid assessment of the results. The temperature of the sample was controlled to within ±0.2°C by a thermostated sample holder, and measured with a calibrated thermal resistor located in a brass block next to the cuvette. A range of temperatures between 12° and 40°C was covered for each sample. In general, data from 16 laser shots were averaged for each measurement; longer exposure of the sample to the intense analyzing light can cause small changes in temperature and possible changes in the sample. In the case of low laser intensity used to avoid excessive excitation of the sample, where the signal-to-noise ratio was poor, results from several (generally 4–5) 16-shot experiments at a fixed temperature were averaged together. The photomultipliers were balanced and the signal averager analogue-to-digital converter base line checked between each measurement. At the higher temperatures and L:P ratios the rotational diffusion coefficient of BR is of the order of $5 \times 10^4\ s^{-1}$, and a sweep time of 0.2 ms was used. This required the measurement of the parallel and perpendicular polarized intensity changes to be made consecutively, and the use of a 579-nm narrow band-pass filter to minimize distortion of the fast initial anisotropy decay by the intense scattered laser pulse.

The maximum resolution time of the apparatus, determined primarily by the laser pulse width and the signal averager sweep time, is ~3 μs.

The $r(t)$ data were transferred to a CDC computer (Control Data Corporation, Sunnyvale, Calif.), where they were analyzed by unweighted nonlinear curve-fitting routines according to the procedure of Marquardt (18).

THEORY

The theoretical time dependence of the anisotropy parameter, $r(t)$, for an asymmetric rotor has been derived by several groups for the case of polarized emission from a chromophore after pulsed excitation (19, 20, 21). Kawato and Kinosita (22) have extended the treatment to the case of membrane proteins in which the partially oriented photo-product is detected by virtue of its absorption properties. If we define $\vec{\mu}_1(\Omega_0, 0)$ as the transition dipole moment for excitation of a molecule oriented along Ω_0 at time zero in the laboratory frame, and $\vec{\mu}_2(\Omega, t)$ as the emission or absorption moment of the molecule oriented along Ω at time t, the emission intensity, $I_\parallel(t)$, or absorption change, $\Delta A_\parallel(t)$, at time t detected parallel to the exciting polarization along the laboratory z-axis (Fig. 1) is proportional to (19, 20)

$$\int P(t)\,[\vec{\mu}_1(\Omega_0, 0) \cdot \hat{\mathbf{z}}]^2\, G(\Omega_0, 0; \Omega, t)\,[\vec{\mu}_2(\Omega, t) \cdot \hat{\mathbf{z}}]^2\, d\Omega d\Omega_0, \tag{2}$$

where $P(t)$ is the probability that the molecule remains excited at time t, $G(\Omega_0, 0; \Omega, t)$ is the probability that the molecule reorients from Ω_0 at time zero to Ω at time t, $\hat{\mathbf{z}}$ is the unit vector along the laboratory z-axis and the expression is averaged over all orientations.

In the case of ground-state depletion, transient absorption changes are detected near the excitation wavelength, the same transition moment being involved in both steps, provided the absorption band corresponds to a single electronic transition. The change in absorbance $\Delta A_\parallel(t)$, is now taken to be proportional to the probability that a molecule oriented along Ω at time t would have absorbed light polarized parallel to z if it had been in the ground state multiplied by the probability that it is not in the ground state, having been excited at time zero

when it was oriented along Ω_0. Analogously to Eq. 2 this may be written

$$\int P(t)\,[\vec{\mu}_1(\Omega_0, 0)\cdot\hat{z}]^2\,G(\Omega_0, 0; \Omega, t)\,[\vec{\mu}_1(\Omega, t)\cdot\hat{z}]^2\,d\Omega d\Omega_0. \quad (3)$$

The derivation of $\Delta A_\parallel(t)$ is then the same as for emission, with the added simplification that the excitation and measuring transition moments are identical. This is an important factor in the quantitative analysis of anisotropy curves since the number of unknown physical parameters is reduced. $\Delta A_\perp(t)$ is derived in a similar way by considering the probability of light absorption perpendicular to z. Calculation of the anisotropy parameter according to Eq. 1 for absorption depletion then gives $r(t)$ as a function of transition moment orientation and rotational diffusion coefficients directly analogous to that for emission anisotropy.

In general the solution to the asymmetric rotor problem yields a sum of five exponentials in the formula for $r(t)$ (19). This complexity may be reduced in the present case by some assumptions concerning the likely arrangement of an integral membrane protein embedded in the lipid bilayer (see Fig. 2). The diffusion coefficients characterizing motion about three orthogonal axes are assumed to be largely determined by the anisotropy of the membrane. In fact chemical labeling experiments (23, 24) suggest that proteins do not tumble across the membrane. If there is no rotational motion about the in-plane axes we may put $D_2 = D_3 = 0$; $D_1 = D_\parallel$; the expression for $r(t)$ becoming (4, 22)

$$r(t) = 1.2\sin^2\theta\cos^2\theta\exp(-t/\phi_\parallel) + 0.3\sin^4\theta\exp(-4t/\phi_\parallel) + 0.1\,(3\cos^2\theta - 1)^2 \quad (4)$$

where $\phi_\parallel = 1/D_\parallel$ is the rotational relaxation time (1) and θ is the orientation of the transition dipole moment with respect to the membrane normal (Fig. 2). The situation where some motion about the in-plane axes is allowed has been treated by Kinosita et al. (25), as a

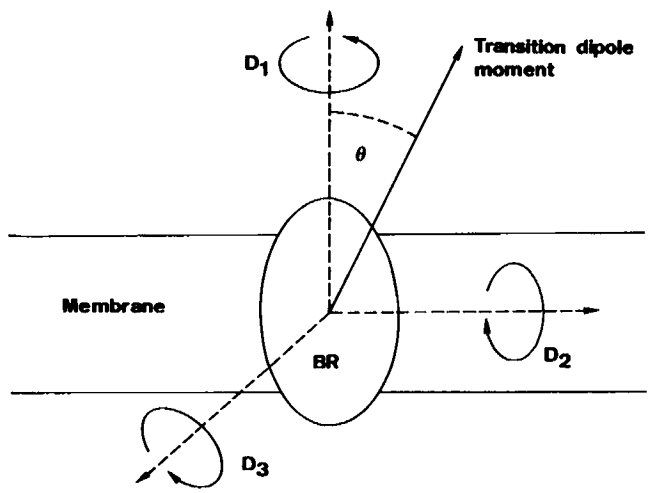

FIGURE 2 Model for bacteriorhodopsin embedded in a lipid bilayer membrane, showing rotational diffusion coefficients about axes normal to the plane of the membrane (D_1) and in the plane (D_2, D_3). θ is the orientation of the transition dipole moment used for excitation and measurement.

"wobbling-in-cone" model, though this may be more appropriate for proteins anchored in the membrane by a small hydrophobic segment.

RESULTS AND DISCUSSION

Fig. 3 shows a series of $r(t)$ curves for BR in DMPC vesicles at a molar L:P ratio of 161 over the temperature range 12°–31°C. It is interesting to note that the protein mobility is not completely frozen out even at several degrees below the pure lipid gel-liquid crystal phase transition temperature (23°C), in accord with previous findings, from a variety of physical

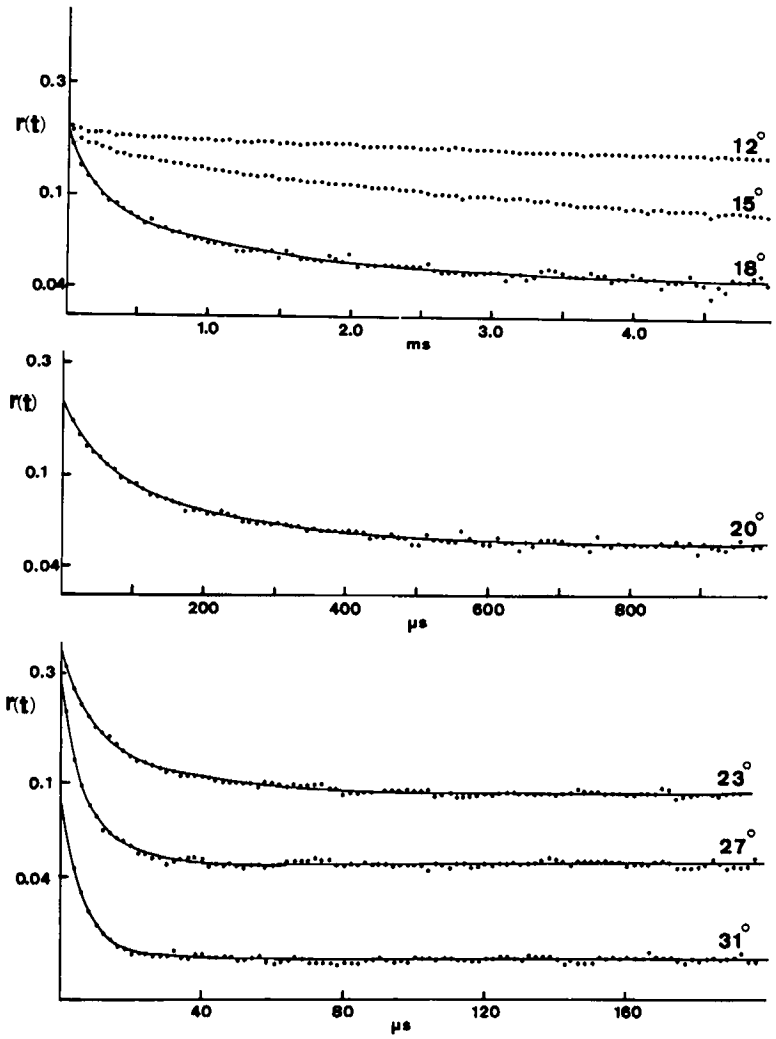

FIGURE 3 Anisotropy decay curves for bacteriorhodopsin in DMPC vesicles at a molar L:P ratio of 161. The points are the experimental data, the solid lines are the best fits of Eq. 7 (see text). 23° and 31°C curves have been displaced vertically for clarity.

methods, on the effect of integral proteins on lipid structure (26–30). The decays become increasingly faster as the temperature is raised and above ~19°C (and for other samples of L:P ratio ~90 and greater) a time-independent residual anisotropy $r(\infty)$ is reached, consistent with Eq. 4. At L:P ratios of ~50 and less, however, no constant anisotropy is reached within 5 ms, even at 37°C, which suggests immobilization of a fraction of BR or formation of large rotating species. Previous measurements on the rotational diffusion of BR in DMPC and DPPC, together with x-ray diffraction and circular dichroism (CD) studies, indicated that, at L:P ratios of ~40 and less, protein aggregates are formed (12) even at temperatures above the lipid phase transition. Our data agree with these observations, the decays in $r(t)$ showing that the aggregates are small enough to have appreciable rotational diffusion, compared with the complete immobilization in the purple membrane (31) where the L:P ratio is ~12.

The possibility that the anisotropy decays are caused by vesicle tumbling is ruled out by several factors. The slow dialysis procedure used for reconstitution yields vesicles of the order of 0.3–0.5 μm diameter, as observed by electron microscopy (12), corresponding to rotational correlation times of 3.5–16 ms in water at 20°C. At temperatures for which there is a rapid decay in $r(t)$ the residual anisotropy $r(\infty)$ reaches a steady value over ~1 ms, incompatible with unrestricted vesicle tumbling which would reduce $r(t)$ to zero. A more quantitative analysis of the decay curves (q.v.) shows that the decay times vary by at least one order of magnitude between 20° and 25°C, whereas the viscosity of water changes by a factor of 1.13.

A decay in $r(t)$ would also be caused by motion of the chromophore, either independently of the protein, or together with a small segment of protein (22). For immobilized BR in the two-dimensional lattice of purple membrane, however, the anisotropy is constant over at least 1 ms and we have observed a value for $r(t)$ of 0.37 when reducing the incident laser intensity with neutral density filters, whereas Dr. K. Kinosita finds a value 0.395 ± 0.007 (personal communication). These values are close to the theoretical maximum of 0.4, which shows that the retinal is held quite rigidly in the protein.

Curve Fitting to a General Multiexponential Decay

We first note that the theoretical expression for $r(t)$ may in practice be modified by a combination of several factors (22, 32). Excitation of a nonnegligible fraction of chromophores, and depolarizations due to light scattering (33) and instrumental factors all combine to reduce $r(t)$. We take this into account by use of the experimental factor $f(A)$, which we assume to be time-independent (22), so that

$$r(t)_{\text{exp}} = f(A)\, r(t)_{\text{theoret}}. \tag{5}$$

As noted above, measurements on a purple membrane suspension show that it is possible to obtain values of $f(A)$ close to 1 by reducing the laser excitation intensity. To improve the signal-to-noise ratios, however, we generally used higher laser intensities, giving values of $r(0)$ for the vesicle samples between 0.2 and 0.3.

A further reduction in $r(t)$ would be produced by a difference in orientation between exciting and measuring transition moments (32), both of which are measured within the broad visible absorption band of BR. The 30-nm separation between the two moments does not appear to be important, however, since, again for purple membrane, we observe no change in $r(t)$ within experimental error, as the measuring wavelength is varied throughout the

absorption band, consistent with the assumption that a single transition moment is involved in both photoselection steps. A similar result was obtained by Heyn et al. (34), who found that the static linear dichroism of oriented purple membrane was wavelength independent throughout the visible absorption band.

Eq. 4 describes the anisotropy decay for a single rotating species, whereas CD measurements indicate that appreciable protein aggregation occurs in these reconstituted systems below the lipid phase transition, even at L:P ratios as high as 150 (12). When a number of different-sized rotating species are present, $r(t)$ will be given by the weighted sum of equations of the form of Eq. 4, i.e.,

$$r(t) = f(A) \sum_{i=1}^{N} c_i \left[A_{1i} \exp\left(-t/\phi_{\parallel i}\right) + A_{2i} \exp\left(-4t/\phi_{\parallel i}\right) + A_{3i}\right], \tag{6}$$

where c_i is the weight fraction of aggregate i and A_{1i}, A_{2i}, and A_{3i} are the relevant trigonometric pre-exponentials from Eq. 4. The analysis of such decay curves, if only a few specific aggregates of different dimensions are present, together with monomers, would involve a multiexponential analysis, a notoriously difficult procedure even with precise data (35, 36). Instead we have attempted, as a first approach, to fit the data with the more general Eq. 7

$$r(t) = P_1 \exp\left(-t/T_1\right) + P_2 \exp\left(-t/T_2\right) + P_3, \tag{7}$$

using a nonlinear least-squares minimization procedure (18) to obtain the best fit provided by the five independent parameters P_1, P_2, P_3, T_1, T_2. The advantage of this approach is apparent if we assume that the transition dipole moments have a fixed orientation with respect to the membrane plane, independent of the aggregation state. Then,

$$r(t) = f(A)\left[A_1 \sum_{i=1}^{N} c_i \exp\left(-t/\phi_{\parallel i}\right) + A_2 \sum_{i=1}^{N} c_i \exp\left(-4t/\phi_{\parallel i}\right) + A_3\right], \tag{8}$$

since

$$\sum_{i=1}^{N} c_i = 1.$$

Comparing Eqs. 7 and 8 we can equate the pre-exponential terms $f(A)A_3$ and P_3, and the initial anisotropies $f(A)(A_1 + A_2 + A_3)$ and $P_1 + P_2 + P_3$, which gives

$$(P_3/P_1 + P_2 + P_3) = (A_3/A_1 + A_2 + A_3) = m = 0.25\,(3\cos^2\theta - 1)^2,$$

$$\text{or } \theta = \cos^{-1}\left(\frac{1 \pm 2\sqrt{m}}{3}\right)^{1/2}, \tag{9}$$

so that for data that show a constant residual anisotropy the values of P_1, P_2, and P_3 may be used to estimate the transition dipole moment orientation and hence the retinal orientation, since the transition dipole responsible for the visible absorption spectrum of BR lies along the all-*trans* polyene chain of retinal. If a single rotating species is the main contributor to $r(t)$ we would hope that the ratio of time constants in Eq. 7 would be 4, and that they would give a reliable estimate of the rotational relaxation time $\phi_{\parallel}$ (see Eq. 4).

Eq. 7 gives a good fit to the experimental decay curves at temperatures >15°C and for all L:P ratios. Lower temperature data were not fitted because of the very slow decay times, which might overlap with vesicle tumbling effects on the longer time scans. As a quantitative goodness-of-fit parameter we use the sum-of-square residuals, defined as (18)

$$s^2 = \sum_{i=1}^{N} \frac{[r_i(t) - r(t)]^2}{N - n},$$

where N is the number of data points and n is the number of parameters. For 16 laser-shot experiments s^2 generally lies between 4×10^{-6} and 1.4×10^{-6}, and in the range 1×10^{-6}–0.3×10^{-6} for greater signal averaging. The examples shown in Fig. 3 typify the kind of fit obtained. There are no large systematic deviations between the curves and the experimental points, even at several degrees below the pure lipid phase transition. This reflects the lack of constraint imposed on the curve fitting by the use of five independent parameters, so that the expected multiexponential decay curves can be accomodated by just two exponentials.

TIME CONSTANTS Fig. 4 shows the temperature variation of the time constants, T_1 and T_2, given by the best fits of Eq. 7 to the data for two representative L:P ratios. It should be emphasized that the large flexibility of the curve-fitting routine allows the pre-exponential parameters to vary in a way that compensates for extreme values of T_1 and T_2. Thus, it is

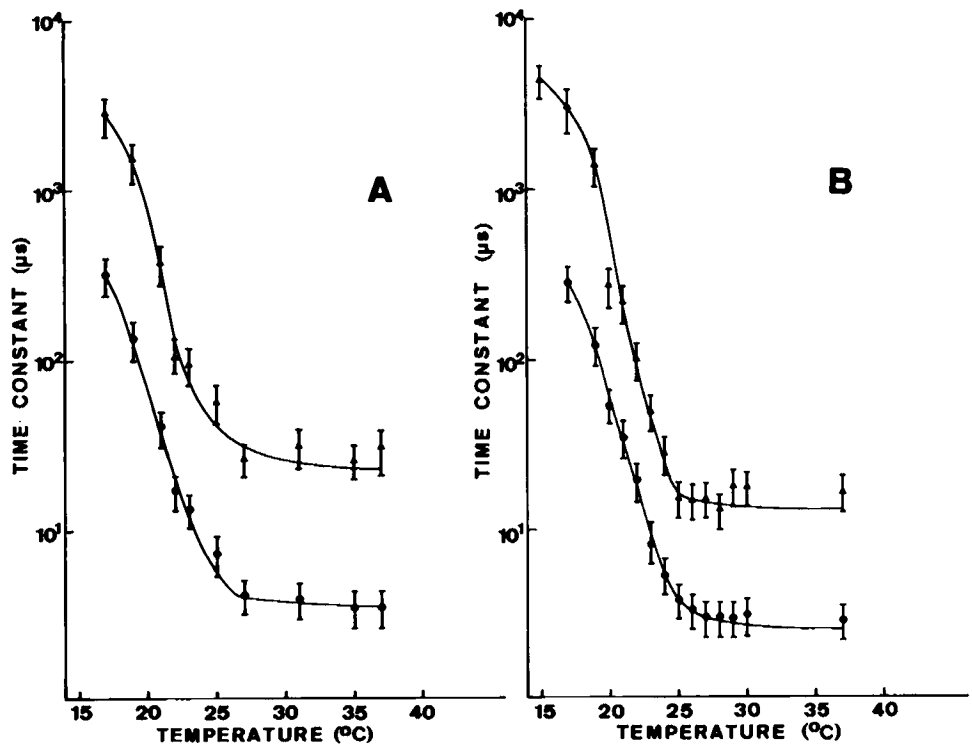

FIGURE 4 Time constants T_1 (▲) and T_2 (●) from curve fitting Eq. 7 to the experimental data, as functions of temperature for molar L:P ratios of 89 (*A*) and 212 (*B*).

possible that the best fit is obtained with, e.g., a very large T_1 and a correspondingly small P_1, which may be physically unrealistic compared with the general trends as a function of temperature. Furthermore, the curve fitting is dependent on the scan time used through the effective weighting of different regions of the digitized decay curve, according to the number of points involved. Where different scan times have been used at a single temperature, decay times have been averaged in Fig. 4. In spite of these limitations, the curves illustrate the general changes in protein mobility as the temperature is raised through the phase transition. In each case the time constants decrease by about two orders of magnitude between 17° and 25°C, further temperature rises resulting in relatively small changes. The rapid decreases in protein rotation as the temperature is lowered are not due simply to reduced lipid fluidity; protein aggregation occurs below the phase transition as a consequence of reduced protein solubility in the lipid (12, 30). The rotational diffusion coefficient varies as the square of the cross-sectional area of protein in the membrane plane (37), so that a rapid decrease in mobility is expected for larger protein units. For example, trimeric protein clusters in a close-packed array would have a rotational diffusion coefficient ~4.6 times smaller than the monomer.

In general, the ratio of time constants T_1:T_2 is greater than the value of 4 expected for a single component from Eq. 4, particularly at the lower temperatures. This ratio lies in the range 10–20 for the lowest L:P ratio, 51, at all temperatures (15°–45°C), whereas for the more dilute protein samples <24°C the range is roughly 6–12, these values illustrating the flexibility of the curve fitting and the multiple exponential nature of the decay curves. Above 24°C the average ratio is ~6. The broadening of the lipid phase transition, as detected by the protein, has been observed before in this (30, 38) and other single lipid systems (26), and has aroused much interest lately in terms of the perturbation of lipid structure by integral proteins.

TRANSITION MOMENT ORIENTATION Calculated values of m from the best-fit parameters P_1, P_2, and P_3 are listed in Table I for several L:P ratios. In each case only data for

TABLE I
TRANSITION MOMENT ORIENTATION AND MINIMUM TEMPERATURES FOR MONODISPERSED BR IN DMPC VESICLES

Molar L:P ratio	m*	θ‡	Temperature§
		(°)	(°C)
89	0.195	79.02	37
136	0.190	78.50	28
161	0.186	77.55	25
179	0.187	77.80	25
212	0.196	77.64	25
237	0.191	77.73	25
Averages:	0.191 ± 0.026‖	78 ± 2¶	

*Geometric factor defined in Eq. 7.
‡Transition moment orientation (in degrees) defined in Eq. 4.
§Minimum temperature for monodispersed BR according to fit of Eq. 4 (all ±1°C).
‖Mean and standard deviation of 62 observations.
¶Mean and standard deviation of 55 observations.

temperatures above the nominal (i.e., pure lipid) phase transition were used, to try to ensure that a constant residual anisotropy had been reached. There is no temperature dependence of m over the range measured, and individual values were averaged together to give the final results. m also appears to be independent of L:P ratio, and the final averaged value of 0.191 ± 0.026 corresponds to an angle of 78° ± 3° or 38° ± 1.5°, depending on the particular root taken in Eq. 9. These figures are in close agreement with those found earlier (34), although

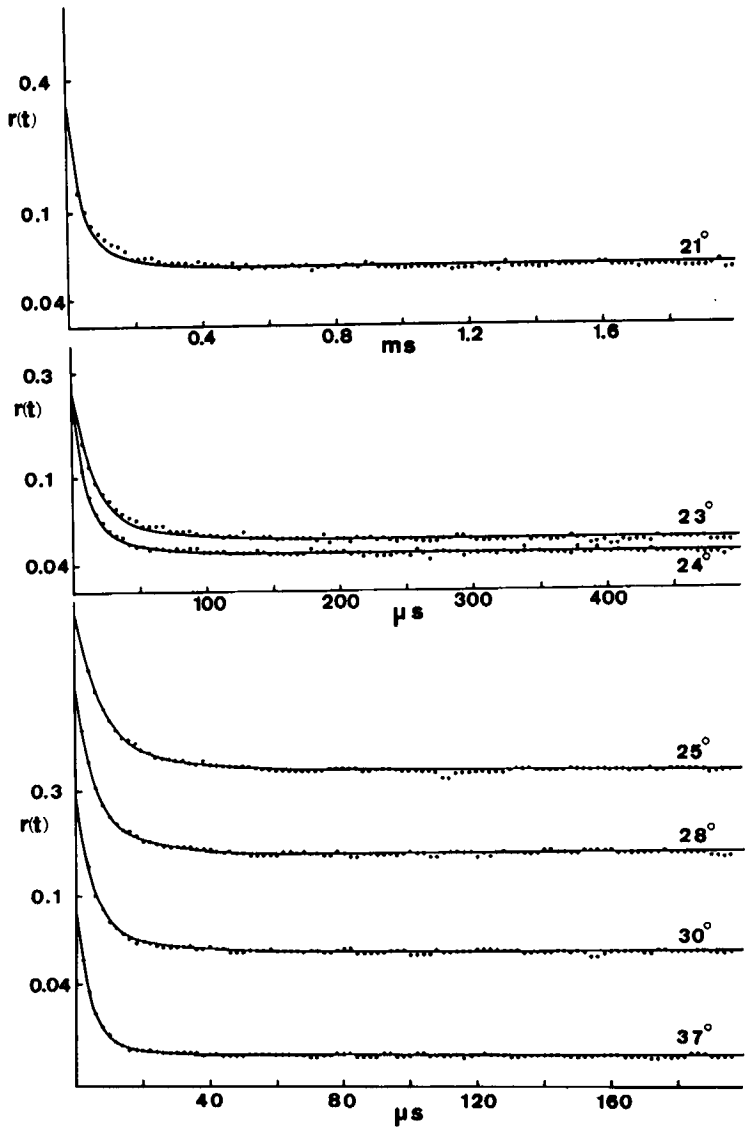

FIGURE 5 Experimental anisotropy decay curves (points) and best fit curves of Eq. 4 (solid lines) for bacteriorhodopsin in DMPC vesicles at a molar L:P ratio of 212. 25, 28, and 37°C curves have been displaced vertically for clarity.

those data were obtained without signal averaging and computer curve fitting. Of the two possible angles we assume that the correct one is 78° ± 3°, since this is closer to the values obtained by linear dichroism measurements on oriented purple membrane (11, 34, 39, 40). A curve-fitting analysis of absorption and CD curves of purple membrane (41) also supports the choice of the higher angle, although a recent structural study casts some doubt on the validity of the CD analysis (42). The possibility that there are substantial differences in the orientation of the chromophore in the purple membrane and in the reconstituted system have been discussed previously (34). It seems unlikely that a gross structural rearrangement takes place on incorporation of the protein in a lipid bilayer in view of the similarities in CD spectra, x-ray diffraction patterns, and proton pumping activity between the reconstituted and native BR (12, 38), although, as we shall discuss later, the small difference between this angle and that from measurements on purple membrane does appear to be significant. Further analysis of the decay curves, discussed in the following sections, in fact removes the ambiguity of the above method of determining the chromophore orientation.

Rigorous Testing of Model of Protein Rotation

Although the analysis of anisotropy decay curves in terms of Eq. 7 provides a useful insight into the general rotational mobility of BR in lipid bilayers, and may be used to estimate the chromophore orientation, it does not provide a stringent test of the theory of protein rotation represented by Eq. 4. For example, Eq. 7 fits the data very well irrespective of the aggregation state of the protein, which reflects the ability of such an equation to accommodate even multiple exponential curves. In those cases where a single component is thought to be present, the procedure does not necessarily give reliable physical parameters, since it has sufficient freedom to continue varying these parameters to obtain the best fit, independently of the

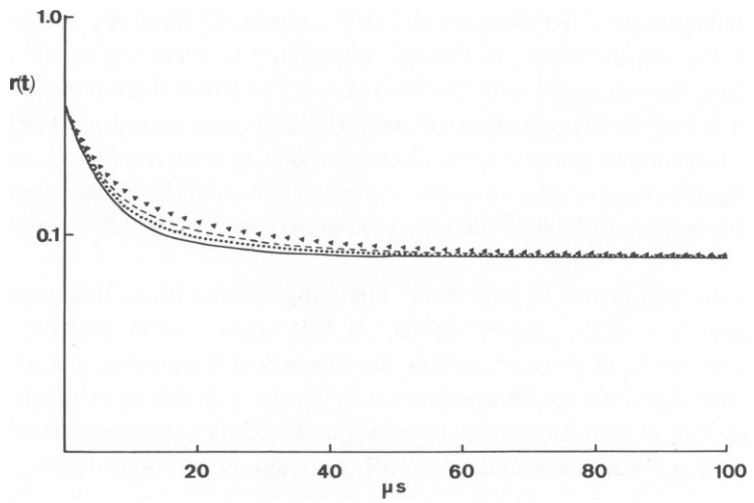

FIGURE 6 Simulated anisotropy decay curves, according to Eq. 4, for a protein with rotational relaxation time of 15 μs in a mixture with varying amounts of a larger rotating species with a relaxation time of 75 μs. —, 100% 15-μs component; ·, 95%; --, 90%; ◀, 80%. Transition moment orientation, 78°.

proposed functional relationships between them. Curve fitting with a fixed time constant ratio of 4 imposes some constraint on the procedure, but still allows the pre-exponentials to vary freely and to provide good fits over a wide temperature range.

As a more rigorous test of the theory we have attempted curve fitting Eq. 4 to the experimental data, with the modification that the curves are reduced by the multiplicative instrument factor $f(A)$. Thus, we took as variable parameters in the curve fitting $f(A)$, θ and ϕ_1. Data for the samples of L:P ratio >80 were analyzed, the general results being typified by the curves in Fig. 5 for a sample with L:P ratio of 212. In this case, at ≥25°C the data are well fitted by the exact theoretical Eq. 4. Comparing the goodness-of-fit parameter, we find in general s^2 is only 20–50% larger for Eq. 4 than it is for Eq. 7. In contrast, <25°C there are clearly systematic deviations between the best-fit curve and the experimental points. In fact <20°C the fitting routine fails to give as close a fit as shown in Fig. 5 for 21° and 23°C. Instead the fit gradually approaches a solution giving $\theta = 90°$, corresponding to a rather high s^2, generally an order of magnitude larger than for the good fits of Fig. 5.

The systematic deviations of Eq. 4 from the data at the lower temperatures indicate the presence of more than one rotating species. Fig. 6 shows simulated anisotropy curves calculated from Eq. 4 for a protein with a rotational relaxation time of 15 μs, in a mixture with varying amounts of a slower component with relaxation time a factor of 5 larger. The presence of relatively small amounts of a second slower component is clearly sufficient to cause significant deviations from the single component decay curve.

Results similar to those in Fig. 5 were obtained for other samples, except that the temperature at which the equation began to fit well varied with L:P ratio. In fact for the sample with L:P ratio of 84 the typical systematic deviations shown in Fig. 5 for 21° and 23°C persisted up to 40°C, which suggests that at this and higher protein concentrations some aggregation occurs independently of the lipid state. Table I lists the temperatures above which Eq. 4 fits the data well, with no systematic deviations, for the various L:P ratios. In all cases, below these temperatures, the theoretical curves appear to miss out a slower decaying component of the experimental anisotropy, although the relatively small discrepancies between the experimental points and the fitted curves just below these temperatures suggest that probably <5% of the BR is aggregated above the lipid phase transition. The temperatures listed in Table I should not be regarded as sharp divisions between completely monomeric and partially aggregated protein, since they are to some extent subjective quantities. Rather they are guides to the conditions under which the protein may be considered essentially monomeric.

Our results are significant in two ways. First, they demonstrate that under conditions favoring rotation of a single species, namely at L:P ratios >~100, and for temperatures sufficiently above the lipid phase transition, the theoretical description of a protein rotating about an axis normal to the membrane plane is in accord with the experimental decay data. Second, the attempt to fit anisotropy decays by Eq. 4 affords a sensitive test for the state of protein aggregation. Previous estimates of BR aggregation in reconstituted systems (12), based on the measurement of exciton coupling in the visible spectrum, have indicated that above a L:P ratio of ~40 there is no detectable aggregation above the lipid phase transition. The higher sensitivity of the present curve-fitting analysis, however, suggests that some aggregation persists up to a L:P ratio of ~100, even above the phase transition. It is probable

that the small fraction of aggregated BR indicated by our measurements gives rise to an exciton contribution to the visible CD that is not detectable under the intrinsic monomeric BR CD curve (43), especially when sensitivity is reduced by light scattering. It should also be remembered that only specific aggregation is detected by exciton effects in the CD spectra, the possibility of nonspecific aggregation (e.g., short-lived randomly associated clusters) cannot be ruled out.

The relationship between the aggregation state and activity of BR has been of some interest lately, particularly in view of the characteristic two-dimensional lattice formed by the protein in its native purple membrane (44). Thus, although Dencher and Heyn (38) have shown that the monomeric protein pumps protons with an efficiency similar to that of the aggregated state, a reduction is observed in light-dark adaption of monomeric BR in lipid vesicles, compared with the crystallised protein in purple membrane or well below the phase transition in the reconstituted system (12, 45). Similarly, the cooperative nature of the reconstitution with retinal of bleached purple membrane (14) suggests that interactions between BR molecules play an important role in determining the structure and properties of the chromophore. Results from the present study also indicate a significant change in the chromophore orientation upon disaggregation of the lattice into monomers, as we discuss below.

TRANSITION MOMENT ORIENTATION Table I lists the angles obtained from data for which Eq. 4 provided a good fit with no systematic deviations. No significant dependence of θ on temperature or L:P ratio is observed and the values for each protein concentration are averaged to give a final angle of 78° ± 2° in very close agreement with the value obtained by use of Eq. 7. The extraction of an accurate angle from the experimental data with Eq. 4 is more satisfactory than the method of Eq. 7 in two respects. First, the latter method depends on

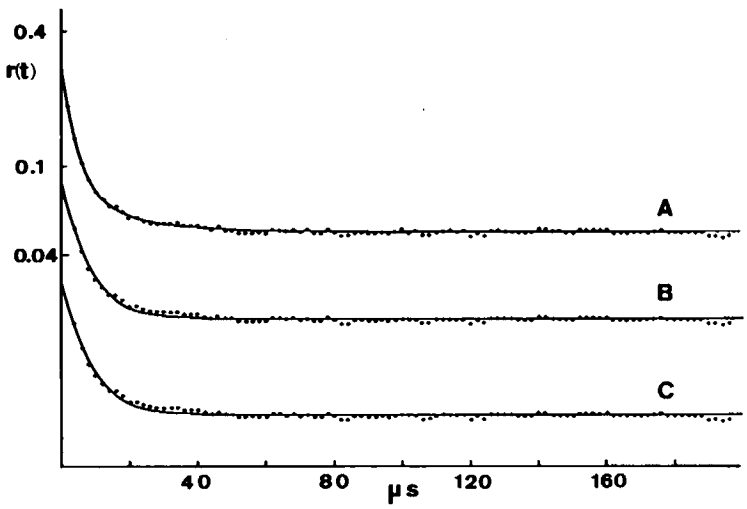

FIGURE 7 Examples of best fits (solid lines) to experimental anisotropy decay curves (points) for Eq. 4, $\theta = 77°$ (*A*); Eq. 4, $\theta = 36°$ (*B*); and Eq. 11, single exponential plus constant (*C*). The experimental curve is for a sample of molar L:P ratio of 212, at 28°C. Curves *B* and *C* have been displaced vertically for clarity.

an accurate determination of $P_1 + P_2 + P_3$ that is identical to $r(0)$. This value is highly dependent on the initial behaviour of the decay curve, and, in view of the possible distortion of this portion of $r(t)$ at high resolution times, can be subject to errors that are reproduced in m. This is particularly true when the use of Eq. 7 yields two time constants whose ratio is much greater than 4. Eq. 4 imposes a much greater constraint on the two exponentials available to fit the data, and the final angle is less subject to errors in a small region of the decay curve. Also the use of Eq. 7 is ambiguous in general, in that m corresponds to two angles. Eq. 4 likewise has two regions of the variable parameter θ for which s^2 is a minimum for the BR/DMPC system, at ~78° and 38°, and in fitting the data it is necessary to choose a starting value for θ involving an inevitable bias towards one of the solutions. The results presented in Table I were obtained with a starting value of 75°, although the results are independent of the starting angle in the range 60°–85°. We have also investigated the best fits obtained with an initial angle of 38°, close to that recently proposed by Hoffmann et al. (46). As illustrated in Fig. 7 for a typical example, in all cases where a good 78° solution exists, the corresponding fit in the 38° region is inferior. The respective s^2 parameters for the best fit angles of 77° and 36° for the example depicted in Fig. 7 are 1.171 and 2.702×10^{-6}, and the mismatch of the lower angle fit shows that this form of Eq. 4 is not capable of describing the particular time dependence of $r(t)$. The reason for this becomes apparent if we look at the relative sizes of the pre-exponentials in Eq. 4 for the two regions. For an angle of 78°, the pre-exponential of the slower decay, A_1, is 0.05, compared with 0.27 for A_2, whereas for $\theta = 38°$, A_1 and A_2 are 0.28 and 0.04, respectively. The curve-fitting results show that the anisotropy decays conform more closely to a major fast decay and minor slow component, whereas forcing the slower decay to dominate results in significant deviations from the experimental points.

We believe that the difference in transition moment orientation found here for monomeric BR, and that found from measurements on the native purple membrane is significant. Although the precision of our result almost overlaps one of the values obtained from linear dichroism, 71 ± 4° (34), various other estimates of θ all give values lower than ours (11, 39, 40, 42), which suggests that random errors alone cannot explain the discrepancy. The differences in chromophore behavior between aggregated and monomeric protein noted earlier tend to support this view, and the possibility that packing of protein into a crystalline lattice can impose sufficient conformational constraint to change slightly the chromophore orientation is not unreasonable. It is of course possible that the reconstitution procedure itself causes a shift in the retinal position, independent of the state of protein aggregation. A useful test of this possibility would be to measure the rotational motion of well defined aggregates of BR, e.g., chemically cross-linked trimers (47), and derive a value for θ. Our result together with the fact that monomeric BR pumps protons with high efficiency (38) may have implications for the various models of proton pumping that have been recently proposed (48–51).

The effect on our determination of θ caused by restricted motion about the in-plane axes, such as in the wobbling-in-cone model (25, 52), has been discussed previously (1), this motion tending to randomize further the transition dipole moment and to reduce the $r(\infty)$ parameter, leading to an angle smaller, not larger, than that from static linear dichroism measurements. This argument and the good fit of Eq. 4 to the experimental data under

appropriate conditions strongly indicate that even restricted wobbling about the in-plane axes is negligible.

ROTATIONAL DIFFUSION COEFFICIENTS The derivation of accurate rotational diffusion coefficients from the anisotropy decay data is more difficult than the determination of the chromophore orientation because the decays are at the limit of time resolution of the apparatus, and the time constant parameter in the curve fitting is more dependent on the initial fast decay than is the angle parameter. Nonetheless, reasonable estimates of the diffusion coefficient are possible for the data obtained by more extensive signal averaging, as illustrated in Fig. 8, which shows the diffusion coefficients as a function of temperature (from the good fits of Eq. 4) for various L:P ratios. Although a regular increase in rotational diffusion is observed between 25° and 27° for two of the samples, the limited precision of the results tends to disguise any further variation in protein mobility at higher temperatures. In fact D would not be expected to change very rapidly once the lipid is completely fluid. The fluorescence anisotropy of diphenylhexatriene in DMPC, for example, has a rather small temperature dependence over this range, although in that case both the motion and order of the lipid are of importance (28). The present results are at variance with an earlier suggestion (16) that the rotational diffusion coefficient of the monomeric protein varies by a factor of 50 on changing the L:P ratio from 22 to 150. This conclusion was based on measurements of reconstituted BR/DMPC vesicles at 25°C and at sufficiently high protein concentrations for aggregation effects to be important, in all but one sample. The analysis of the present data using Eq. 7 also gives a variation in time constants at 25°C of one order of magnitude over a L:P range of 51–250, but it is more likely that this is due to protein aggregation effects. The direct comparison of rotational diffusion coefficients over a wide range of protein concentrations is difficult at present, since at the high concentrations the protein does not rotate as a single species, and at low concentrations the rotation may become too fast to measure accurately. Fig. 8 shows that the differences in rotational mobilities at the three protein concentrations are close to the error limits of our measurements. The general trend, however,

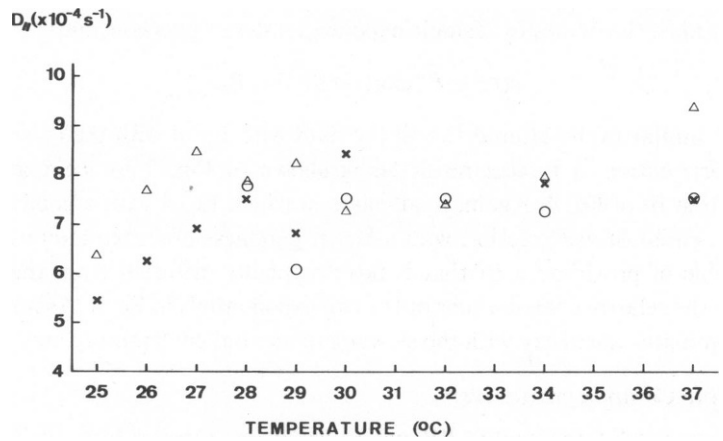

FIGURE 8 Rotational diffusion coefficient $D_{\parallel}$ derived from best fits of Eq. 4 to the anisotropy decay curves, as a function of temperature, at molar L:P ratios of 136 (○), 179 (×), and 212 (△).

does show that protein concentration is a factor determining rotational diffusion, probably through some kind of protein effect on membrane viscosity. We expect that improved instrumental time resolution will enable a more definitive statement to be made concerning the effects of protein concentration.

If we neglect the possible small dependence of $D_\parallel$ on temperature and L:P ratio, we note that all values in Fig. 8 fall within the range 5–10 $\times$ 10^4 s^{-1}, corresponding to a relaxation time, $\phi_\parallel = 15 \pm 5$ μs. The dimensions of the BR monomer are 45 $\times$ 35 $\times$ 25 Å (44). Using the relationship (37) for a cylinder of radius a and height h,

$$D_\parallel = \frac{kT}{4\pi a^2 h \eta}, \tag{10}$$

and taking the larger cross-sectional dimension for a = 17.5 Å, and h = 45 Å, we calculate that the membrane viscosity η experienced by the protein is 3.7 $\pm$ 1.3 P, between 25° and 37°C. These values for $\phi_\parallel$ and η should provide a useful calibration for other systems. It is likely that the viscosity of fluid lipid bilayers is not strongly dependent on lipid composition, so that large variations in $\phi_\parallel$ for different proteins probably reflect differences in diameter or restrictions on free diffusion due to protein-protein interactions. Thus, for rhodopsin in rod outer segment disc membranes (3), $\phi_\parallel = 20 \pm 10$ μs at 20°C, which indicates that the protein is monomeric and its cross-sectional diameter in the plane of the membrane is not very different from that of BR.

Measurements on erythrocyte membranes reveal that band 3 protein is present in two populations with different rotational mobilities (53). One population with $\phi_\parallel$ in the millisecond time range has restricted motion, owing to interaction with cytoskeletal proteins, whereas a second population has $\phi_\parallel \sim 200$ μs. The difference between this relaxation time and that of BR in our model system is likely to be due to the larger molecular weight of band 3 (~90,000) and the fact that it is present as dimers or higher oligomers.

CURVE FITTING TO A SINGLE EXPONENTIAL DECAY As a further check on our interpretation of the experimental decay curves in terms of anisotropic protein rotation we have attempted to fit the curves by a single exponential decay plus constant:

$$r(t) = P_1 \exp(-t/T) + P_3. \tag{11}$$

The results are similar to the attempts to fit the data with Eq. 4 with the lower angle for the chromophore orientation, a typical result being shown in Fig. 7 for comparison with the corresponding best fit of Eq. 4. Again, in all cases in which Eq. 4 gave a good fit to the data, the single exponential fit was inferior, with a larger goodness-of-fit parameter. The fact that Eq. 11 is capable of providing a fit that is not drastically different from the experimental curves is due to the relative contributions of the two exponentials in Eq. 4. As noted previously, the A_2 term dominates the decay with the slower exponential contributing only ~15%.

Multiple Component Analysis

Although the presence of aggregated BR molecules at low temperatures or high concentrations should provide a good model system for investigating membrane protein aggregation, each rotating species contributes a double exponential decay to $r(t)$, so that the experimental anisotropy curve requires a multiexponential analysis to obtain the orientation and mobility

parameters, as well as the fractions of each species. The difficulties inherent in such procedures have been emphasized by Grinvald and Steinberg (35). In the present case we have attempted to extract consistent parameters from the decay data by some assumptions about the possible state of aggregation in those situations where the single component Eq. 4 just fails to provide a good fit. The deviations from a single component fit caused by small amounts of species with diffusion coefficients only five times smaller than the monomer (Fig. 6) suggests that we might at least rationalize the experimental data in terms of only two components.

Since we are mainly concerned with determining reasonable estimates of the diffusion coefficients and fractions of each species, as a first approach we fixed the orientation of the chromophore transition moment and took as variable parameters the two relaxation times, the fraction of monomer, and the experimental factor $f(A)$. Although as discussed above, monomers and aggregated BR may have slightly different chromophore orientation, use of a single angle instead of two does not affect the general conclusions of our analysis. Good fits to the data were obtained with this procedure but the parameters did not fit into a consistent pattern. Generally, extreme values for one or other time constant were compensated by the fractions involved, similar to the effect noticed in fitting Eq. 7. For the next approach we assumed that the majority of oligomers formed are either dimers, trimers, or tetramers, which on a simple hydrodynamic basis (assuming circular cross-sections and close packing) have relaxation times 4, 4.6, and 5.8 times slower than the monomer. With the relative time constant ratio fixed at 5, the variable parameters used were the fraction and time constant of monomer and the factor $f(A)$. Even with these constraints the results do not provide a consistent physical picture, although the actual fits are very good.

We conclude that at the present level of experimental accuracy curve fitting procedures can demonstrate the existence of multiple components but cannot reliably resolve the contributions of the different components.

CONCLUSIONS

The main conclusions of the curve fitting analyses presented in this paper may be summarized as follows. (*a*) A model in which a single species of BR rotates only around the membrane normal provides an excellent description of the experimental decay curves, provided the L:P ratio is $>\sim 100$ and the temperature is sufficiently above the lipid phase transition. Although other models could conceivably be used to explain the data, the present model is certainly the simplest and the introduction of more complex models does not appear justified at present. (*b*) At lower L:P ratios and temperatures the inability of the model to account for the experimental data can be explained by the presence of BR aggregates. Curve fitting provides a sensitive test of the existence of such aggregates, but resolution of the respective contributions of different-sized aggregates is not possible at the present level of experimental accuracy. (*c*) Determination of the chromophore orientation from the ratio of the final to the initial anisotropy yields two solutions, $\theta = 78 \pm 3°$ and $\theta = 37 \pm 1.5°$. But the best fit to the whole anisotropy decay curve under the conditions specified above in (*a*) shows that the correct solution is $\theta = 78 \pm 2°$. This value is significantly different from the value for the retinal orientation in purple membrane. (*d*) Under the conditions specified above in (*a*), the

rotational relaxation time for bacteriorhodopsin $\theta_{\parallel} = 15 \pm 5$ μs, corresponding to a membrane viscosity of 3.7 ± 1.3 P.

We would like to thank Carmen Zugliani for expert technical assistance.

This work was supported by grants from the Swiss National Science Foundation and the F. Hoffmann-La Roche Stiftung (grant no. 160).

Received for publication 8 November 1980 and in revised form 4 June 1981.

REFERENCES

1. Cherry, R. J. 1979. Rotational and lateral diffusion of membrane proteins. *Biochim. Biophys. Acta.* 559:289–327.
2. Singer, S. J., and G. L. Nicolson. 1972. The fluid mosaic model of the structure of cell membranes. *Science (Wash. D.C.)* 175:720–731.
3. Cone, R. A. 1972. Rotational diffusion of rhodopsin in the visual receptor membrane. *Nature (Lond.).* 236:39–43.
4. Cherry, R. J. 1978. Measurement of protein rotational diffusion in membranes by flash photolysis. *Methods Enzymol.* 54:47–61.
5. Austin, H. A., S. S. Chan, and T. M. Jovin. 1979. Rotational diffusion of cell surface components by time-resolved phosphorescence anisotropy. *Proc. Natl. Acad. Sci. U.S.A.* 76:5650–5654.
6. Moore, C., D. Boxer, and P. Garland. 1979. Phosphorescence depolarization and the measurement of rotational motion of proteins in membranes. *FEBS (Fed. Eur. Biochem. Soc.) Lett.* 108:161–166.
7. Thomas, D. D. 1978. Large scale rotational motions of proteins detected by electron paramagnetic resonance and fluorescence. *Biophys. J.* 24:439–462.
8. Hyde, J. S. 1978. Saturation-transfer spectroscopy. *Methods Enzymol.* 49:480–511.
9. Axelrod, D., D. E. Koppel, J. Schlessinger, E. Elson and W. W. Webb. 1976. Mobility measurement by analysis of fluorescence photobleaching recovery kinetics. *Biophys. J.* 16:1055–1069.
10. Jacobson, K., Z. Derzko, E.-S. Wu, Y. Hou and G. Poste. 1976. Measurements of the lateral mobility of cell surface components in single living cells by fluorescence recovery after photobleaching. *J. Supramol. Struct.* 5:565–576.
11. Stoeckenius, W., R. H. Lozier, and R. A. Bogomolni. 1979. Bacteriorhodopsin and the purple membrane of Halobacteria. *Biochim. Biophys. Acta.* 505:215–278.
12. Cherry, R. J., U. Müller, R. Henderson and M. P. Heyn. 1978. Temperature-dependent aggregation of bacteriorhodopsin in dipalmitoyl- and dimyristoylphosphatidylcholine vesicles. *J. Mol. Biol.* 121:283–298.
13. Lowry, O. H., N. J. Rosebrough, A. L. Farr, and R. J. Randall. 1951. Protein measurement with the folin phenol reagent. *J. Biol. Chem.* 193:265–275.
14. Rehorek, M., and M. P. Heyn. 1979. Binding of all-*trans* retinal to the purple membrane. Evidence for cooperativity and determination of the extinction coefficient. *Biochemistry.* 18:4977–4983.
15. Chen, P. S., Jr., T. Y. Toribara, and H. Warner. 1956. Microdetermination of phosphorous. *Anal. Chem.* 28:1756–1758.
16. Cherry, R. J., U. Müller, and G. Schneider. 1977. Rotational diffusion of bacteriorhodopsin in lipid membranes. *FEBS (Fed. Eur. Biochem. Soc.) Lett.* 80:465–470.
17. Jablonski, A. 1961. Über die Abklingungsvorgänge polarisierter Photolumineszenz. *Z. Naturforsch. A.* 16:1–4.
18. Bevington, P. R. 1969. Data Reduction and Error Analysis for the Physical Sciences. McGraw-Hill, Inc., New York.
19. Ehrenberg, M., and R. Rigler. 1972. Polarized fluorescence and Brownian motion. *Chem. Phys. Lett.* 14:539–544.
20. Belford, G. G., R. L. Belford, and G. Weber. 1972. Dynamics of fluorescence polarization in macromolecules. *Proc. Natl. Acad. Sci. U.S.A.* 69:1392–1393.
21. Chuang, T. J., and K. B. Eisenthal. 1972. Theory of fluorescence depolarization by anisotropic rotational diffusion. *J. Chem. Phys.* 57:5094–5097.
22. Kawato, S., and K. Kinosita, Jr. 1981. Time dependent absorption anisotropy and rotational diffusion of proteins in membranes. *Biophys. J.* 36:277–296.

23. Bretscher, M. 1973. Membrane structure: some general principles. *Science (Wash. D.C.).* 181:622–629.
24. Singer, S. J. 1974. The molecular organisation of membranes. *Annu. Rev. Biochem.* 43:805–833.
25. Kinosita, K., Jr., S. Kawato, and A. Ikegami. 1977. A theory of fluorescence polarization decay in membranes. *Biophys. J.* 20:289–305.
26. Chapman, D., J. C. Gomez-Fernandez, and F. M. Goni. 1979. Intrinsic protein-lipid interactions. *FEBS (Fed. Eur. Biochem. Soc.) Lett.* 98:211–223.
27. Seelig, A., and J. Seelig. 1978. Lipid-protein interaction in reconstituted cytochrome *c* oxidase/phospholipid membranes. *Hoppe-Seyler's Z. Physiol. Chem.* 359:1747–1756.
28. Heyn, M. P. 1979. Determination of lipid order parameters and rotational correlation times from fluorescence depolarization experiments. *FEBS (Fed. Eur. Biochem. Soc.) Lett.* 108:359–364.
29. Owicki, J. C., and H. M. McConnell. 1979. Theory of protein-lipid and protein-protein interactions in bilayer membranes. *Proc. Natl. Acad. Sci. U.S.A.* 76:4750–4754.
30. Heyn, M. P., R. J. Cherry, and N. A. Dencher. 1981. Lipid-protein interactions in bacteriorhodopsin-phosphatidylcholine vesicles. *Biochemistry.* 20:840-849.
31. Cherry, R. J., M. P. Heyn, and D. Oesterhelt. 1977. Rotational diffusion and exciton coupling of bacteriorhodopsin in the cell membrane of *Halobacterium halobium. FEBS (Fed. Eur. Biochem. Soc.) Lett.* 78:25–30.
32. Albrecht, A. C. 1970. The method of photoselection and some recent applications. *Prog. React. Kinet.* 5:301-334.
33. Teale, F. W. J. 1969. Fluorescence depolarization by light scattering in turbid solutions. *Photochem. Photobiol.* 10:363–374.
34. Heyn, M. P., R. J. Cherry, and U. Müller. 1977. Transient and linear dichroism studies on bacteriorhodopsin: determination of the orientation of the 568 nm all-*trans* retinal chromophore. *J. Mol. Biol.* 117:607–620.
35. Grinvald, A., and I. Z. Steinberg. 1974. On the analysis of fluorescence decay kinetics by the method of least squares. *Anal. Biochem.* 59:583–598.
36. Provencher, S. W. 1976. An eigenfunction expansion method for the analysis of exponential decay curves. *J. Chem. Phys.* 64:2772–2777.
37. Saffman, P. G., and M. Delbruck. 1975. Brownian motion in biological membranes. *Proc. Natl. Acad. Sci. U.S.A.* 72:3111–3113.
38. Dencher, N. A., and M. P. Heyn. 1979. Bacteriorhodopsin monomers pump protons. *FEBS (Fed. Eur. Biochem. Soc.) Lett.* 108:307–310.
39. Acuna, A. U., and J. Gonzalez-Rodriguez. 1979. Form dichroism and retinal orientation in bacteriorhodopsin. *An. Quim.* 75:630–635.
40. Korenstein, R., and B. Hess. 1978. Immobilisation of bacteriorhodopsin and orientation of its transition moment in purple membrane. *FEBS (Fed. Eur. Biochem. Soc.) Lett.* 89:15–20.
41. Ebrey, T. G., B. Becher, B. Mao, P. Kilbride, and B. Honig. 1977. Exciton interactions and chromophore orientation in the purple membrane. *J. Mol. Biol.* 112:377–397.
42. King, G. I., P. C. Mowery, W. Stoeckenius, H. L. Crespi, and B. P. Schoenborn. 1980. Location of the chromophore in bacteriorhodopsin. *Proc. Natl. Acad. Sci. U.S.A.* 77:4726–4730.
43. Bauer, P.-J., N. A. Dencher, and M. P. Heyn. 1976. Evidence for chromophore-chromophore interactions in the purple membrane from reconstitution experiments of the chromophore-free membrane. *Biophys. Struct. Mech.* 2:79–92.
44. Henderson, R., and P. N. T. Unwin. 1975. Three-dimensional model of purple membrane obtained by electron microscopy. *Nature (Lond.).* 257:28–32.
45. Casadio, R., and W. Stoeckenius. 1980. Effect of protein-protein interaction on light adaption of bacteriorhodopsin. *Biochemistry.* 19:3374–3381.
46. Hoffmann, W., C. J. Restall, R. Hyla, and D. Chapman. 1980. Protein rotation and chromophore orientation in reconstituted bacteriorhodopsin vesicles. *Biochim. Biophys. Acta.* 602:531–538.
47. Dellweg, H.-G., and M. Sumper. 1978. Selective formation of bacterio-opsin trimers of chemical cross linking of purple membrane. *FEBS (Fed. Eur. Biochem. Soc.) Lett.* 90:123–126.
48. Lewis, A., M. A. Marcus, B. Ehrenberg, and H. Crespi. 1978. Experimental evidence for secondary protein-chromophore interactions at the Schiff base linkage in bacteriorhodopsin: molecular mechanism for proton pumping. *Proc. Natl. Acad. Sci. U.S.A.* 75:4642–4646.
49. Fischer, U., and D. Oesterhelt. 1979. Chromophore equilibria in bacteriorhodopsin. *Biophys. J.* 28:211–230.
50. Honig, B., T. Ebrey, R. H. Callender, U. Dinur, and M. Ottolenghi. 1979. Photoisomerism, energy storage, and charge separation: a model for light energy transduction in visual pigments and bacteriorhodopsin. *Proc. Natl. Acad. Sci. U.S.A.* 76:2503–2507.

51. Crespi, H. L., and J. R. Ferraro. 1979. Active site structure of bacteriorhodopsin and mechanism of action. *Biochem. Biophys. Res. Comm.* 91:575–582.
52. Lipari, G., and A. Szabo. 1980 Effect of librational motion on fluorescence depolarization and nuclear magnetic resonance relaxation in macromolecules and membranes. *Biophys. J.* 30:489–506.
53. Nigg, E. A., and R. J. Cherry. 1980. Anchorage of a band 3 population at the erythrocyte cytoplasmic membrane surface: protein rotational diffusion measurements. *Proc. Natl. Acad. Sci. U.S.A.* 77:4702–4706.